

X-RAY DIFFRACTION DETERMINATION OF STRESSES IN THIN FILMS

T. VREELAND, JR., A. DOMMANN, C.-J. TSAI, AND M.-A. NICOLET
California Institute of Technology, Pasadena, CA 91125

ABSTRACT

This paper presents the methodology employed in the determination of the stress tensor for thin crystalline films using x-ray rocking curves. Use of the same equipment for the determination of the average stress in poly- or non-crystalline thin films attached to a crystalline substrate is also discussed. In this case the lattice curvature of the substrate is determined by measurement of the shift in the Bragg peak with lateral position in the substrate.

Strains in single crystal layers may be measured using Bragg diffraction from the layers and from the substrate or a reference crystal, with the highest strain sensitivity of any known technique. The difference in Bragg angles for a strained and an unstrained crystal is related to the change in d spacing of the Bragg planes, and the elastic strain is related to this angular difference. The separation of two peaks on an x-ray rocking curve is generally not equal to the difference in Bragg angles of two diffracting crystals, so diffractometer measurements must be carefully interpreted in order to obtain x-ray strains in crystalline films (x-ray strains are strains relative to the reference crystal). The unstrained d spacings of the film and the d spacings of the reference crystal must be known to obtain the elastic strains in the film, from which the stress tensor is determined.

INTRODUCTION

Measurement of the separation of peaks on x-ray rocking curves (curves of diffracted intensity vs. angle) is commonly employed in the determination of strains in a thin single crystal layer on a crystalline substrate. The very high strain sensitivity of x-ray measurements was demonstrated by Bonse and Hartmann in Si [1]. Using a large Bragg angle and sensitive x-ray intensity measurement, a strain sensitivity of $10E-8$ was obtained. A strain sensitivity of $\approx 10E-5$ to $10E-4$ is typical using x-ray rocking curves with Bragg angles ≈ 45 degrees.

We consider here the determination of the stresses in single, uniformly strained layers. The analysis of multilayer structures is briefly discussed.

The equipment used for obtaining x-ray rocking curves consists of the following components:

1. An x-ray source

Typically, a sealed x-ray tube is used with a Cu target. Other targets are sometimes employed to access different Bragg angles. More intensity is needed for a single, very thin layer (less than about 20 nm), and a rotating anode or synchrotron source is used.

2. An x-ray monochromator

Typically a $K\alpha$ reflection from one single crystal of high quality is used to reduce the wave length spread of the incident beam to the sample. In this case, the $K\alpha_2$ diffraction may be removed by a slit placed between the monochromator crystal and the sample. Sharp diffraction peaks are needed if high angular resolution is to be obtained. The sharpest diffraction peaks from a sample crystal are obtained when the Bragg angle of a single monochromator crystal and the sample are equal. Use of a multiple crystal monochromator, as suggested by Dumond [2], removes the $K\alpha_2$ and does not cause

peak broadening when the Bragg angles of the monochromator crystal and sample differ. This increases angular resolution at the expense of some x-ray intensity.

3. Sample goniometer

The goniometer should be capable of angular adjustments of the sample with a step size of $\approx 10E-4$ degrees which is useful in some applications. The range of angular adjustments required may exceed 10 degrees for some samples, and a range of ≈ 160 degrees makes the system more versatile.

4. X-ray photon counter

We employ a scintillation crystal (NaI) with a thin Be input window, coupled to a photomultiplier tube, preamplifier, amplifier, single channel analyzer, and pulse counter.

5. Control and recording system

Typical pulse counting times using a sealed x-ray tube source are on the order of 10 s at each angular step, and the diffracted intensity (counts/s) vs. relative goniometer angle is recorded. Digital records of this data permit rapid computer analysis and plotting of rocking curves with the intensities normalized by the incident beam intensity to give the reflecting power, or reflectivity vs. angle.

ANALYSIS OF THE ROCKING CURVE

Uncoupled Crystals

In the analysis of x-ray rocking curves of thin films with thick reference crystals (thin and thick compared to the x-ray absorption length), it is often assumed that the diffraction from a layer is not influenced by neighboring layers, so that the kinematic theory of diffraction may be used for the thin layer or layers, and the dynamical theory for the reference [3]. In general, the peak in diffracted amplitude from a highly perfect reference crystal is shifted from the Bragg angle, θ_{Br} by a small negative increment (about $3.8E-4$ degrees with a plane wave $CuK\alpha_1$ and the 440 Si reflection) [4].

Wave length spread in the incident beam from a single monochromating crystal will generally cause the peak intensity to fall within $1E-4$ of the Bragg angle of the reference crystal. We will assume the peak intensity from the reference crystal is at the Bragg angle θ_{Br} in the treatment in this section.

We also assume that the kinematic theory is applicable, and we will examine this assumption in a subsequent section.

The difficulty in the determination of absolute angles in a rocking curve is avoided when the Bragg peak from a reference crystal of accurately known d spacing is recorded together with the peak from the film. According to the assumptions in this section, the rocking curve is the sum of the intensities diffracting from the reference crystal and the film. We treat first the case where the diffracting planes of both reference crystal and film are parallel. Two distinct peaks will appear on the rocking curve when $\Delta\theta_B = \theta_{Bf} - \theta_{Br}$ is sufficiently large (the subscripts refer to film and reference). The Bragg peak from a single layer decreases in amplitude and increases in width as the layer thickness decreases, and complicates determination of $\Delta\theta_B$ for thin films.

The difference in Bragg angles is related to the d plane spacings of the film and reference by

$$\Delta\theta_B = \sin^{-1}\lambda/2d_f - \sin^{-1}\lambda/2d_r \quad (1)$$

where λ = x-ray wavelength.

The x-ray strain normal to the parallel Bragg planes of the film and reference crystal is found from Eq. 1 to be

$$\epsilon_{x\text{-ray}} \equiv (d_f - d_r)/d_r = \sin\theta_{Br}/\sin(\theta_{Br} + \Delta\theta_B) - 1 \quad (2)$$

For small x-ray strains Eq. 2 reduces to

$$\epsilon_{x\text{-ray}} \approx -\Delta\theta_B/\tan\theta_{Br} \quad (3)$$

Heteroepitaxial films with relatively large x-ray strains are often analysed. The error in $\epsilon_{x\text{-ray}}$, introduced by use of Eq. 3 instead of Eq. 2 for stress-free films with a Si reference and $\text{FeK}\alpha_1$, is shown in Fig. 1. The error is not negligible in the systems with large lattice mismatch such as GaAs on Si.

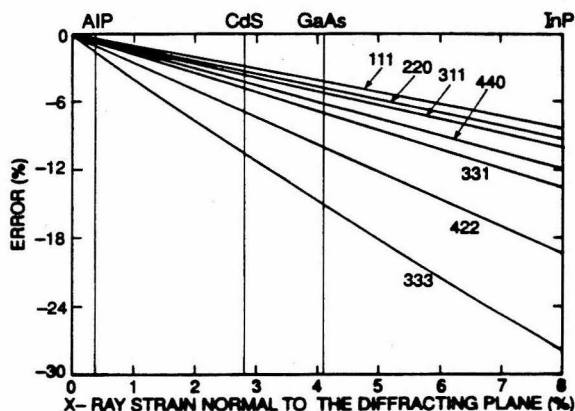


Fig. 1. The error in the x-ray strain for stress-free crystals introduced by the small strain approximation, Eq. 2 using a Si reference crystal and different diffracting planes with $\text{FeK}\alpha_1$.

The x-ray strains must be converted to the strains of elasticity theory in order to employ Hooke's law for determination of the stresses. The elasticity normal strains are given by

$$\epsilon_{\text{elasticity}} \equiv (d_f - d_{fo})/d_{fo} = (\epsilon_{x\text{-ray}} + 1)d_r/d_{fo} - 1 \quad (4)$$

where d_{fo} is the film d spacing when it is stress-free.

Direct measurement of the angle $\Delta\theta$, between the maximas of the reference peak and the film peak on a rocking curve may differ from $\Delta\theta_B$ due to a) an asymmetric reference peak, as discussed above, b) a dynamical interaction of the x-ray waves when the film and reference crystals are in contact (coupled), as discussed below, c) tilt between the film and reference diffracting planes, and d) peak overlap. The overlap effect is removed when the diffracted intensity from the reference crystal is subtracted from the rocking curve.

Crystals have a multiplicity of planes suitable for x-ray diffraction so normal strains in different directions in a film may be found. The strain normal to the film surface is particularly easy to determine when the diffracting planes are parallel to that surface (symmetric diffraction). This is one principal strain when the axes of principal stress and strain coincide.

Additional normal strains can then be measured using planes inclined to the surface (asymmetric diffraction), from which the other two principal strains are found. Unequal strains normal and parallel to the film surface cause tilt of the asymmetric Bragg planes in the film relative to those in the reference crystal (which is a function of the angle between these film planes and the film surface), so that the film diffraction peaks are shifted by this tilt in addition to the shift due to the d spacing change [5]. Additional tilt between the diffracting planes of the film and a substrate may result in the growth process, so the total tilt should be measured when asymmetric diffraction is used as discussed below.

Asymmetric Rocking Curves from Uncoupled Crystals

The x-ray geometry for a non-skew asymmetric diffraction in the diffraction plane (the plane containing the incident and diffracted beams) is shown in Fig. 2. (In a skew diffraction the normal to the diffracting plane does not lie in the diffraction plane.) When there is tilt between the film and reference crystals, this tilt may be found by obtaining two rocking curves, one as shown in Fig. 2 and one with the diffraction vectors reversed. This reverses the sign of the angular shift of the film diffraction peak due to the tilt. The tilt angle is then one-half of the difference in peak shifts, $\Delta\theta_1 - \Delta\theta_2$, in the two rocking curves, while the strain is related to one-half of the sum of the two peak shifts. The x-ray strain normal to the diffracting plane is then

$$\epsilon_{x\text{-ray}} = \sin\theta_{Br} / \sin(\theta_{Br} + \Delta\theta_i \pm \xi(\psi_r)) - 1 \quad (i = 1, 2) \quad (5)$$

where $\xi(\psi_r)$ = the tilt angle and the minus sign is used when the diffraction vectors are as shown in Fig. 2 (incident x-rays at angle $\theta - \psi_r$ from the sample surface), and the plus sign is used for $\theta + \psi_r$ incidence.

When the x-ray strains are small Eq. 5 reduces to

$$\epsilon_{x\text{-ray}} \approx -(\Delta\theta_i \pm \xi(\psi_r)) / \tan\theta_{Br} \quad (6)$$

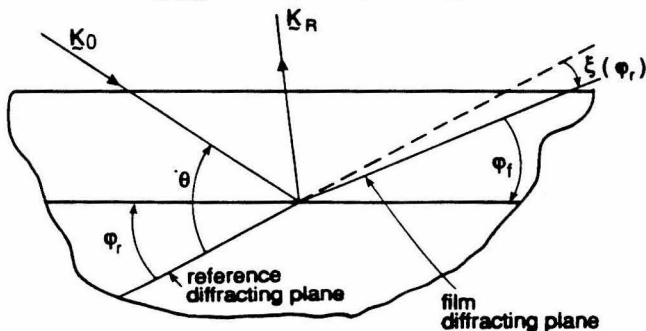


Fig. 2. X-ray geometry for an asymmetric, non-skew reflection with a tilt, $\xi(\psi_r)$ between a film and reference crystal. The incident beam is K_0 , the diffracted beam is K_R , and the angles between the diffracting planes in the film and reference crystal and the film surface are ϕ_f and ϕ_r respectively.

Procedure for Determination of Principal Strains

The principal strain directions in a strained epitaxial film are dictated by the crystallography of the film and substrate. We treat here the case

where both crystals are orthotropic in the surface planes or have perpendicular planes of mirror symmetry which are also perpendicular to the film surface, such as {111}, {100}, and {110} planes of cubic crystals. The surface plane and the mirror planes, or any other two orthogonal planes perpendicular to the surface in the orthotropic case, are then planes of principal strain. Rocking curves are obtained from two different diffracting planes whose normals lie in a principal plane. Normal strains, perpendicular to the two diffraction planes are determined from these rocking curves together with the tilt between film and substrate (using Eqs. 5 or 6). The principal x-ray strains in the plane of the measured normal strains are then given by

$$\epsilon_{\text{perpendicular}} = (\epsilon_{\psi_2} / \sin^2 \psi_2 - \epsilon_{\psi_1} / \sin^2 \psi_1) / (\cot^2 \psi_2 - \cot^2 \psi_1) \quad (7)$$

and

$$\epsilon_{\text{parallel}} = (\epsilon_{\psi_2} / \cos^2 \psi_2 - \epsilon_{\psi_1} / \cos^2 \psi_1) / (\tan^2 \psi_2 - \tan^2 \psi_1) \quad (8)$$

where ϵ_{ψ_1} and ϵ_{ψ_2} are the x-ray strains normal to the two diffracting planes and perpendicular and parallel refers to the film surface. To maximize the strain sensitivity, one of the diffracting planes should have the minimum possible ψ and the other the maximum. When the film surface is a diffracting plane, $\psi_1 = 0$, and

$$\epsilon_{\text{perpendicular}} = \epsilon_{\psi_1} \quad (9)$$

and

$$\epsilon_{\text{parallel}} = (\epsilon_{\psi_2} - \epsilon_{\psi_1} \cos^2 \psi_2) / \sin^2 \psi_2 \quad (10)$$

Repetition of these steps using rocking curves from planes whose normals lie in the third principal plane provides a consistency check on $\epsilon_{\text{perpendicular}}$ and gives the third principal strain. For epitaxial films grown on surfaces of lower symmetry, for example surfaces tilted with respect to {100}, {111}, or {110} cubic crystal faces, additional diffracting planes must be used in order to determine the principal strains and their directions.

Examples

Strain measurement using rocking curves of epitaxial InGaAsP layers of differing alloy composition on InP substrates have proven useful in finding the growth conditions which avoid premature failure of the laser due to high strain in the active alloy layer. The rocking curve of Fig. 3a shows the substrate peak and the peak from a single alloy layer of the composition which gives the desired frequency in a laser structure. However, the strain in a laser with a single layer of this alloy causes failure after a few lasing periods. The rocking curve in Fig. 3b is from a five layer laser structure with three layers of the same alloy as that of the single layer in Fig. 3a. The layers below the active layer have been decoupled from the substrate by interface dislocations to reduce layer strains in the five layer structure by over a factor of two and premature failure in this structure is avoided.

The strain tensor in a heteroepitaxial film of (001) Si on (1102) sapphire was found using symmetric and asymmetric rocking curves from the Si film and from a piece of Si wafer as a reference, fixed to the surface of the film (with a viscous grease) [6]. In this case, the x-ray strain is also the elasticity strain. Fig. 4 shows the superimposed symmetric rocking curves taken with the diffraction vectors reversed from which the perpendicular strain and one component of the tilt between film and reference was obtained.

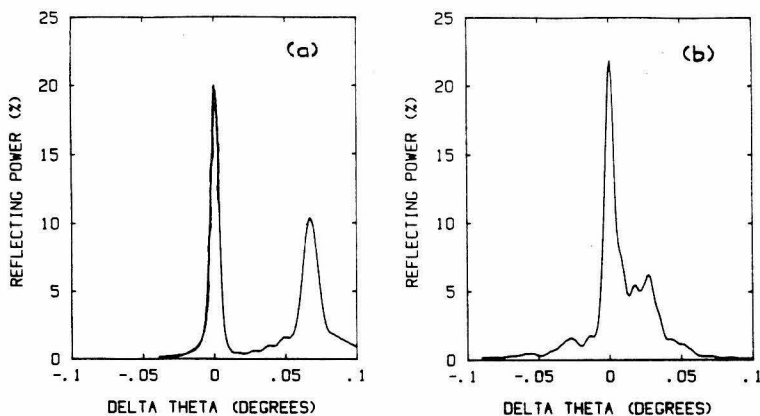


Fig. 3. Symmetric rocking curves of the 004 reflection from a) a single layer of InGaAsP on InP with the alloy content adjusted to that required for the desired wavelength in a laser structure, and from b) a five layer laser structure with the alloy content in three of the layers the same as that in a). Significant relaxation of strain in the active layer of the laser structure by interface dislocations is indicated by the positions of the peaks in a) and b), $\text{FeK}\alpha_1$ radiation.

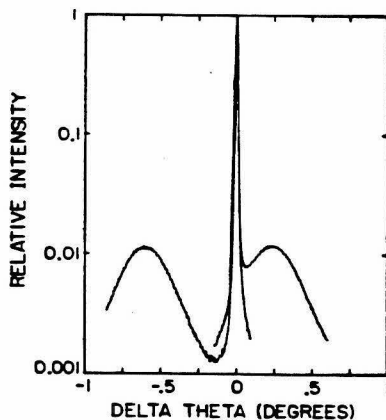


Fig. 4. Superimposed symmetric 004 rocking curves from a (001) Si film grown on (1102) sapphire using a stress-free Si reference crystal attached to the surface of the film. The diffraction vectors are reversed in the two topographs (sample was rotated 180 degrees about the normal to the film). The reference crystal peak is at $\Delta\theta = 0$, the difference in peak shifts is equal to twice the tilt angle between film and reference, and the sum of the two peak shifts is equal to $2\Delta\theta_B$, $\text{FeK}\alpha_1$ radiation.

Coupled Crystals

The dynamical theory of x-ray diffraction must be used to properly take into account the boundary condition between coupled crystal layers (layers in intimate contact) [7]. It has been shown that the peak positions in this case are not equal to those for uncoupled layers [8]. While the difference is small when the layer thickness is sufficiently large, it is not negligible for thin layers with small strains. The ratio of $\Delta\theta_{\text{peaks}}$ to $\Delta\theta_B$ is shown in Fig. 5 for $\text{Al}_{0.25}\text{Ga}_{0.75}\text{As}$ films of thickness from 200 to 1000 nm on GaAs calculated using the dynamical theory and $\text{FeK}\alpha_1$. The peak separation in the calculated curve becomes significantly smaller than $\Delta\theta_B$ as the layer thickness decreases. This example together with more extensive calculations for different epitaxial systems indicate that the ratio approaches unity with increasing film thickness and with increasing strain for a layer of given thickness [9]. Therefore, simulation of the rocking curve using the dynamical theory should be employed to find the x-ray strain in thin layers with small strains.

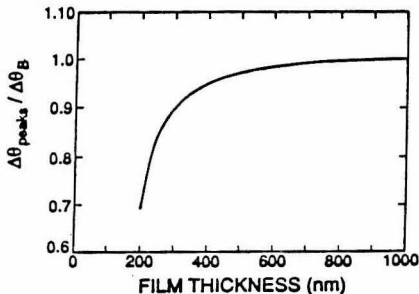


Fig. 5. The ratio of $\Delta\theta_{\text{peaks}}$ calculated by the dynamical theory using $\text{FeK}\alpha_1$ and 004 diffraction, to $\Delta\theta_B$ as a function of the thickness of coherent $\text{Al}_{0.25}\text{Ga}_{0.75}\text{As}$ layers 200 to 1000 nm thick on (001) GaAs.

MULTILAYER STRUCTURES

The stresses in multilayer structures may be investigated by matching their rocking curves to those obtained by computer simulation. Examples in epitaxial systems and in ion implanted crystals are given in [10], where the structures were modeled by uniform layers of different thickness, x-ray structure factor, and strain (using kinematic or dynamical x-ray calculations). While a layer model which gives a calculated rocking curve that matches well with the experimental curve is not a unique solution, we generally know enough about the actual structure to model it accurately.

A recent extension of the rocking curve technique has been reported which gives the promise of extending it to the study of very thin layers, such as the active layer in quantum laser structures. When a thin crystal epilayer is confined between two multilayer structures which have a mirror symmetry about the confined layer, a phase shift in the x-rays diffracting from the confined layer occurs. A small kink on the flank of the principal peak from the confining layers then may be observed (11,12). The kink position and amplitude depends upon the product of the strain in the confined layer and its thickness. Computer simulation of coherent model systems with large lattice mismatch (such as $\text{In}_{0.37}\text{Ga}_{0.63}\text{As}$ with 100 nm $\text{Al}_{0.4}\text{Ga}_{0.6}\text{As}$ confining layers on GaAs, which have perpendicular x-ray strains of 3.9% and 0.08% respectively) show a kink when the confined layer is thicker than about one nanometer. The active layer thickness in a quantum well laser affects the threshold voltage and band gap and it can be determined by x-ray analysis in highly perfect structures.

AVERAGE STRESS MEASUREMENT

Curvature Measurements and Film Stresses. Films on a Crystalline Substrate

Stresses in a film on a crystalline substrate cause bending of the substrate in the plane of the film, and the bending may be related to the average stresses in the plane of the film and the elastic properties of the sample. With a translation stage added to the rocking curve sample holder, the shift in the substrate Bragg peak may be measured at different lateral positions on a film grown on a crystalline substrate. The average principal stresses in polycrystalline or non-crystalline films can then be found from the peak shifts. When the film is less than about one x-ray absorption length thick, the measurements may be made using either the film side or the back side of the substrate.

In order to obtain good angular sensitivity for the peak shifts, the sample stage should be capable of translations of several mm with rotation less than $1E-4$ degrees. We have found a sample stage supported by four thin parallel flexures, when translated by a motor mike pushing on the elastic center of the flexure system, meets this requirement.

The radius of curvature of the substrate crystal in the diffraction plane is given by

$$R = \Delta s / \Delta \theta \quad (11)$$

where Δs = separation of the positions on the sample which gave substrate diffraction peaks separated by $\Delta \theta$, and

$\Delta \theta$ = angular shift of the substrate diffraction peak.

A radius of curvature of 1 km gives a $\Delta \theta$ of $1E-4$ degrees with a Δs of about 1.7 mm.

For a sample free of tractions, the radius of curvature is related to the total force in the film and the elastic properties of the sample. When the film is thin compared to the substrate thickness, the elastic properties of the substrate, its thickness, and the bending moment in the substrate determine its principal radii of curvature. We will consider the case for elastically orthotropic or orthorhombic substrate plates here, specifically cubic crystals with {001}, {111}, or {011} surfaces, and give an example where {001} Si is used.

The principal radii of curvature are then [13]

$$R_1 = (h^3 / 12 S'_{11}) / (M_1 - M_2 S'_{12} / S'_{11}) \quad (12)$$

and

$$R_2 = (h^3 / 12 S'_{22}) / (M_2 - M_1 S'_{12} / S'_{22}) \quad (13)$$

where h = the sample thickness (\approx substrate thickness).

S'_{11} , S'_{22} , S'_{12} = the substrate elastic constants referred to the

orthorhombic symmetry directions, and

M_1 , M_2 = bending moments producing R_1 and R_2 .

Each bending moment is directly related to the corresponding force per unit length in the film, and the average stresses in the film are found when the film thickness is known, giving

$$\sigma_1 = 2M_1 / ht \text{ and } \sigma_2 = 2M_2 / ht \text{ for } h \gg t. \quad (14)$$

where t = film thickness.

The stresses, in terms of the measured radii are then

$$\sigma_1 = (h^2 / 6t) (S'_{22} / R_1 + S'_{12} / R_2) / (S'_{11} S'_{22} - S'^2_{12}), \quad (15)$$

and

$$\sigma_2 = (h^2 / 6t) (S'_{11} / R_2 + S'_{12} / R_1) / (S'_{11} S'_{22} - S'^2_{12}). \quad (16)$$

Stresses in Films on (100), (111), and (110) Substrates

The stresses given above are for plates in pure bending, and it is assumed that the plates are strain-free with no films on them and have no temperature gradients in them. Plates with [100] normals have {100} principal planes, so that

$$S'_{11} = S'_{22} = S_{11} = (c_{11} + c_{12})/[(c_{11} - c_{12})(c_{11} + 2c_{12})], \text{ and} \quad (17)$$

$$S'_{12} = S_{12} = -c_{12}/[(c_{11} - c_{12})(c_{11} + 2c_{12})]. \quad (18)$$

where c_{11} , c_{22} , c_{12} = elastic moduli referred to the cubic directions.

Plates with (111) normals which are free of shear stress on their surfaces are orthotropic in bending, and

$$S'_{11} = S'_{22} = [c_{11}/\{(c_{11} - c_{12})(c_{11} + 2c_{12})\} - 1/2c_{44}] / 2, \text{ and} \quad (19)$$

$$S'_{12} = [(c_{11} - 4c_{12})/\{(c_{11} - c_{12})(c_{11} + 2c_{12})\} - 1/2c_{44}] / 6. \quad (20)$$

A plate with (110) surfaces in pure bending has principal curvatures in [001] and $[\bar{1}10]$ directions, which are the directions of σ_1 and σ_2 respectively. The elastic coefficients in this case S'_{11} and S'_{12} are given by Eqs. 17 and 18, and

$$S'_{22} = c_{11}/[(c_{11} - c_{12})(c_{11} + 2c_{12})] + 1/4c_{44}. \quad (21)$$

The substrate 400 diffraction peak from a traction-free (100) Si crystal, measured at two points with $\Delta s = 4$ mm is shown in Fig. 6a. The $\Delta\theta$ determined by fitting the measured points with a Gaussian curve is less than the probable error in the fitting of $1E-4$ degrees. The same result is obtained from both faces of the crystal, indicating that the translation stage rotates less than $1E-4$ degrees with 4 mm of translation. Alternating layers of Ti and Ni were evaporated on 0.2 mm thick (100) substrates, with a total metal thickness of about 40 nm. The substrate peaks measured on one of these samples, at two points 4 mm apart on the film side, is shown in Fig. 6b. The probable error in the peak shift determined by Gaussian fitting is less than $1E-4$ degrees.

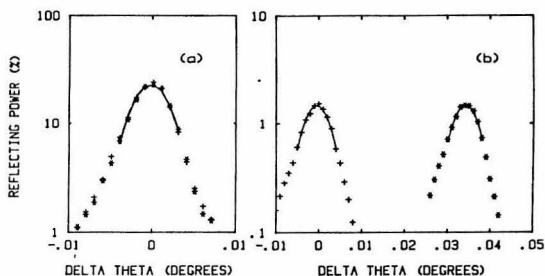


Fig. 6. The 400 $FeK\alpha_1$ diffraction peaks from regions 4 mm apart on (100) Si for a) a stress free crystal, and b) on a crystal with alternating evaporated layers of Ti and Ni. Different plotting symbols are used for the different regions, and Gaussian curves fit to the data from each region are shown as solid lines.

Samples prepared with varying thicknesses of the Ti and Ni layers, of 8 to 12 periods each, were analysed for film stresses after some room temperature ageing. The results are shown in Fig. 7, and indicate an interesting effect of the average concentration in the multilayer [14].

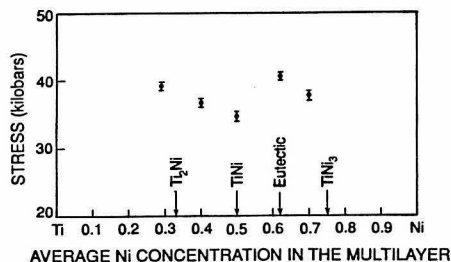


Fig. 7. Stresses determined by substrate curvature measurements in samples with alternating layers of Ti and Ni on (100) Si as a function of the average concentration in the multilayer. The ratio of the total thickness of the layers to the substrate thickness was about 1/7000.

ACKNOWLEDGEMENTS

The authors wish to thank Prof. D. S. Wood for checking our calculations of the elastic constants. This work was sponsored by the Semiconductor Research Corporation and the National Science Foundation, Materials Research Groups, grant no. 8811795.

REFERENCES

1. V. Bonse and I. Hartmann, *Z. Kristallogr.* **156**, 256 (1981).
2. J. W. M. DuMond, *Phys. Rev.* **52**, 812 (1973).
3. V. S. Speriosu, *J. Appl. Phys.* **52**, 6094 (1981).
4. W. H. Zachariasen, *Theory of X-ray Diffraction in Crystals*, (Wiley, New York, 1945).
5. V. S. Speriosu and T. Vreeland, Jr., *J. Appl. Phys.* **56**, 1591 (1984).
6. Thad Vreeland, Jr., *J. Mater. Res.* **1**, 712 (1986).
7. C. R. Wie, T. Tombrello, and T. Vreeland, Jr., *J. Appl. Phys.* **59**, 3742 (1986).
8. P. F. Fewster and C. J. Curling, *J. Appl. Phys.* **62**, 4154 (1987).
An incorrect boundary condition was used in the calculations which introduced a small error in their results. The correct boundary condition is given in [7].
9. C. R. Wie, Y. Choi, J. F. Chen, T. Vreeland, Jr. and C.-J. Tsai, (unpublished) to be presented at the Spring MRS meeting, April 1989.
10. T. Vreeland, Jr. and B. M. Paine, *J. Vac. Sci. Technol.*, **A4**, 3151 (1986).
11. X. Chu and B. K. Tanner, *Appl. Phys. Lett.*, **49**, 1773 (1986).
12. C. R. Wie, to appear in *J. Appl. Phys.*
13. R. F. S. Hearmon, *Applied Anisotropic Elasticity*, (Oxford University Press, 1961).
14. Unpublished results, T. Vreeland, Jr., R. B. Schwarz, and K. H. Samwer.